# *magu* is required for germline stem cell self-renewal through BMP signaling in the *Drosophila* testis

**Qi Zheng**[a,c], **Yiwen Wang**[b,*], **Eric Vargas**[b], and **Stephen DiNardo**[b,c,§]

[a]Department of Biology, School of Arts and Sciences, University of Pennsylvania, Philadelphia, PA 19104, USA

[b]Department of Cell and Developmental Biology, Perelman School of Medicine, University of Pennsylvania, Philadelphia, PA 19104, USA

[c]Penn Institute for Regenerative Medicine, University of Pennsylvania, Philadelphia, PA 19104, USA

## Abstract

Understanding how stem cells are maintained in their microenvironment (the niche) is vital for their application in regenerative medicine. Studies of *Drosophila* male germline stem cells (GSCs) have served as a paradigm in niche-stem cell biology. It is known that the BMP and JAK-STAT pathways are necessary for the maintenance of GSCs in the testis (Kawase et al., 2004; Kiger et al., 2001; Schulz et al., 2004; Shivdasani and Ingham, 2003; Tulina and Matunis, 2001). However, our recent work strongly suggests that BMP signaling is the primary pathway leading to GSC self-renewal (Leatherman and DiNardo, 2010). Here we show that *magu* controls GSC maintenance by modulating the BMP pathway. We found that *magu* was specifically expressed from hub cells, and accumulated at the testis tip. Testes from *magu* mutants exhibited a reduced number of GSCs, yet maintained a normal population of somatic stem cells and hub cells. Additionally, BMP pathway activity was reduced, whereas JAK-STAT activation was retained in mutant testes. Finally, GSC loss caused by the *magu* mutation could be suppressed by overactivating the BMP pathway in the germline.

## Keywords

*magu*; BMP; Germline stem cell; Stem cell niche; *Drosophila* testis

## Introduction

Adult stem cells contribute a steady source of new cells to maintain many tissues, including skin, blood, intestine and the germline. A key hallmark of these cells is their ability to generate new stem cells as well as differentiating progeny. Maintaining a balance between self-renewal and differentiation is thereby crucial for tissue homeostasis. Studies on diverse stem cell systems have demonstrated that the stem cell niche, or the local tissue

microenvironment, provides important extracellular cues for controlling this balance (Li and Xie, 2005). Understanding the modulation of these cues and the signaling pathways they act upon is central focus of current research.

The *Drosophila* male germline system has emerged as an exemplary model for studying the biology of adult stem cells (Fuller and Spradling, 2007). Unlike most mammalian systems, cells that comprise the niche have been conclusively identified, as have several niche signals that serve to maintain the stem cell pool (Kawase et al., 2004; Kiger et al., 2001; Leatherman and DiNardo, 2008; Leatherman and DiNardo, 2010; Schulz et al., 2004; Shivdasani and Ingham, 2003; Tulina and Matunis, 2001). The apical tip of the testis is occupied by a group of tightly packed, terminally differentiated somatic cells, called hub cells (Hardy et al., 1979). Radially arranged around the hub are two intermingled sets of stem cells. One is a population of germline stem cells (GSCs), and the other is a population of somatic stem cells, called cyst stem cells (CySCs).

Generally, each GSC division is oriented (Yamashita et al., 2003), such that one daughter remains adjacent to the hub and to CySCs, thereby retaining stem cell character, while the other is pushed away, and will initiate differentiation as a gonialblast (Gb). After four rounds of mitosis, the Gb generates a cyst of sixteen spermatogonia, which then undergo differentiation into spermatocytes. The division of each CySC is also oriented (Cheng et al., 2011), such that one daughter cell remains attached to the hub, and likely retains stem cell identity, while the other daughter, displaced away from the hub, becomes a differentiating cyst cell. The cyst cell daughters withdraw from the cell cycle, and they continue to provide regulatory input to the encysted differentiating germ cells throughout spermatogenesis (Fabrizio et al., 2003; Matunis et al., 1997).

Both hub cells and CySCs serve as a niche for GSCs (Leatherman and DiNardo, 2008; Leatherman and DiNardo, 2010). It has been shown that BMP ligands are expressed from these two types of niche cells, and that they activate the BMP pathway in GSCs (Kawase et al., 2004; Shivdasani and Ingham, 2003). One output of pathway activation is repression of *bag of marbles* (*bam*) in GSCs, which would otherwise drive differentiation (Kawase et al., 2004; Schulz et al., 2004; Shivdasani and Ingham, 2003). Loss of BMP receptors or signal transducers in the GSCs causes de-repression of *bam* and precocious differentiation (Kawase et al., 2004; Schulz et al., 2004; Shivdasani and Ingham, 2003).

The second signaling pathway active in the stem cell niche is the JAK-STAT pathway. Unlike BMPs, Unpaired (Upd), the JAK-STAT ligand, is only expressed from hub cells (Kiger et al., 2001; Tulina and Matunis, 2001). Upd activates the pathway not only in GSCs, but also in CySCs (Kiger et al., 2001; Leatherman and DiNardo, 2008; Leatherman and DiNardo, 2010; Tulina and Matunis, 2001). JAK-STAT activation appears important for adhesion of both GSCs and CySCs to the hub, but is only crucial for self-renewal of the CySCs (Leatherman and DiNardo, 2008; Leatherman and DiNardo, 2010).

Although BMP signaling is required for GSC maintenance, research has heavily focused on JAK-STAT in stem cell self-renewal over the last several years. Part of the reason may be because induction of ectopic GSCs can be achieved by overactivating the JAK-STAT pathway, but not the BMP pathway (Kawase et al., 2004; Kiger et al., 2001; Schulz et al., 2004; Shivdasani and Ingham, 2003; Tulina and Matunis, 2001). However, recent work from our lab demonstrates that the expansion of GSCs is not directly due to activation of JAK-STAT in GSCs, but rather due to JAK-STAT activation in CySCs, and the consequent enhanced expression of BMP ligands from CySCs (Leatherman and DiNardo, 2010). Therefore, it now appears that BMP is the primary pathway leading to GSC self-renewal, and it is imperative to dissect out the mechanism by which BMP signaling maintains GSCs.

In a previous microarray experiment performed by our lab, *CG2264* was identified as a gene exhibiting transcriptional enrichment in cells near the testis tip (Terry et al., 2006). Subsequently, Li and Tower reported that global ectopic expression of *CG2264*, which they named *magu*, led to an increased life span in both sexes and an increase in the fecundity of older females (Li and Tower, 2009). More recently, Vuilleumier et al. identified *CG2264*, naming it *pentagone* (*pent*), and demonstrated, through loss- and gain-of-function experiments, that it was required for the proper graded activation of the BMP pathway during wing patterning (Vuilleumier et al., 2010).

Here, we will use *magu* as the name for *CG2264*. We report that *magu* is expressed from hub cells, and functions as a BMP modulator that specifically affects the GSC population. Our work emphasizes the importance of BMP signaling in male GSC maintenance.

## Material and methods

### Fly strains

Fly lines used were: *magu*frgII-LacZ, *magu*frgIIΔS-LacZ, and UAS-V5-*magu* (George Pyrowolakis, University of Freiburg, Germany), *nanos*-Gal4:VP16 (Erica Selva, University of Delaware, USA), *upd*-Gal4 (Erika Matunis, John Hopkins University, USA), *upd*-Gal4 UAS-GFP (Erika Bach, New York University, USA), *bam*-GFP (Dennis McKearin, UT Southwestern, USA), UAS-*tkv*A (Kristi Wharton, Brown University, USA). The following transposable insertion lines were from the Exelixis Collection at Harvard Medical School: *magu*$^{d00269}$ (FBti0053977), *magu*$^{e00439}$ (FBti0046433), and *magu*$^{f02256}$ (FBti0050490). All other stocks including *magu*$^{KG02847b}$ (FBti0023111) were provided by the Bloomington Stock Center or generated in this study. Flies were grown at 25°C unless noted.

### Generation of magu mutants

A precise excision of *magu*$^{e00439}$ was isolated as described to generate a revertant, while deletion I was made using FRT/FLP-mediated hybrid element insertion starting with the PiggyBac insertions *magu*$^{d00269}$ and *magu*$^{f02256}$ (Parks et al., 2004). The resulting lines were verified by PCR. An identical allele was independently made and reported previously (called pent2; Vuilleumier et al., 2010). To obtain mutants with potentially larger deletions, the P-element transposon KG02847b was remobilized, and new lines exhibiting a wing vein phenotype over the *magu*$^{e00439}$ allele were selected out. Inverse PCR was used to identify the endpoints of the resulting deletions. The deletions begin in the KG element, and extend to genomic coordinate 5966K for line 76 (reported in Table 1), 5987K for line 123, 6325K for line 166, 5988K for line 862 (Flybase, release before Feb. 2010).

### Generation of an anti-Magu antibody

A 6xHis epitope tag (Qiagen pQE vector) was fused N-terminally to residues 36–214 of Magu. The resulting protein was purified from soluble whole bacterial extracts, using Ni-NTA beads (Qiagen), and injected into rabbits. The crude sera were preabsorbed 1:5000 against fixed *w1118* testes at 4°C for 24 hrs. Titration of this antibody revealed that the preabsorbed 1:5000 dilution gave the best signal-to-noise ratio.

### Plasmids

*magu* sequence was amplified via PCR from BDGP cDNA LD30894, and cloned using Gateway recombination methods (Invitrogen) into either a pUAST-Myc or pUAST-GFP destination vector (developed by Terence Murphy, DGRC). Transgenic flies were produced using standard germline transformation techniques.

### In situ hybridization

*In situ* hybridization on testes using digoxigenin-labeled antisense RNA probes was performed as previously described (Terry et al., 2006).

### Immunostaining

Immunostaining for gonads and adult testes was performed as previously described except 1×PBS was substituted for Buffer B (Leatherman and DiNardo, 2010). The following antibodies were used: mouse anti-lacZ (1:10,000, Promega), rat anti-E-Cadherin (1:20, DSHB), rabbit anti-Magu (1:5000), rabbit anti-Magu (1:15,000, George Pyrowolakis, University of Freiburg, Germany), goat anti-Vasa (1:400, Santa Cruz), mouse anti-FascIII (1:100, DSHB), mouse anti-α-Spectrin (1:200, DSHB), rabbit anti-Zfh1 (1:5,000, Ruth Lehmann, New York University, USA), chick anti-GFP (1:1000, Molecular Probes), rabbit anti-Stat (1:5000, Erika Bach, New York University, USA), rabbit anti-pMad (1:1000, Carl-Henrik Heldin, Ludwig Institute for Cancer Research, Sweden), mouse anti-Eya (1:20, DSHB) and guinea pig anti-Traffic jam (1:10,000, Dorothea Godt, University of Toronto, Canada). Attempts to visualize pMad in adult testes using anti-pMad generally failed. In one experiment, several testes exhibited clearly positive signals. The example in Fig 5C is from this experiment.

For extracellular staining, testes were dissected in cold Ringer's solution, and incubated for 2 to 3 hrs in cold Ringer's solution containing 2% normal donkey serum and 1:15,000 rabbit anti-Magu (developed by George Pyrowolakis), and washed for 3×20 min in cold Ringer's solution, followed by the standard fixation and immunostaining protocol.

### Imaging and imaging analysis

Images were captured with a Zeiss Axioplan 2 equipped with an apotome. Z-series were analyzed by the AxioVision 4.6 software, except that projection images for Magu (standard staining), α-Spectrin, and pMad (for testes) were created by ImageJ (NIH) software. Various cell types were counted by stepping through optical sections. Excel (Microsoft) was used for statistical analysis. GSC number in *magu* mutants did not fall into a normal distribution, thus the Mann-Whitney test was used to calculate P-value on the VassarStats web site (http://faculty.vassar.edu/lowry/VassarStats.html).

### Mounting fly wings

Wings from adult flies were dissected in methylsalicilate (Sigma, C1705) and mounted in 2:1 Canada Balsam (Sigma, M-6752): methylsalicilate.

### S phase labeling

S phase labeling of testes was performed as previously described (Leatherman and DiNardo, 2010).

## Results

### *magu* is expressed from hub cells

Using *in situ* hybridization, we visualized *magu* mRNA in the hub cells (Fig.1A). In our hands, *in situ* hybridization in testes did not have the resolution and reproducibility usually afforded in other tissues. We always observed signals among small cells clustered at tip (Fig1A, arrowheads), and we concluded that these were hub cells. Due to the technical limitations, we could not rule out the possibility that *magu* is expressed in some somatic cells near the hub (in some CySCs). However, we have not observed any evidence of expression in large-profile cells surrounding the hub. Thus, we are confident that *magu* is

not expressed in germline cells. Interestingly, *in situ* hybridization sometimes suggested that *magu* was expressed only from some hub cells, or to higher degree from some hub cells (Fig 1A, arrowheads).

To more definitively identify which cells express *magu*, we made use of a LacZ reporter line of *magu* (Vuilleumier et al., 2010). This reporter utilizes a 2 kilobase fragment that recapitulates *magu* expression in the developing wing disc (Vuilleumier et al., 2010). In the testis, we observed that *magu* expression was restricted to hub cells as shown by double-labeling with E-Cadherin (Fig. 1B). Interestingly, the reporter was not expressed in all hub cells. It remains possible that some other regulatory region at *magu* drives expression in the remaining hub cells. However, since some of our *in situ* preparations also suggested non-homogenous expression from hub cells, perhaps *magu* is under temporal or spatial control, and under repression by BMP signaling (Vuilleumier et al., 2010). Indeed, mutation of Mad/Medea/Schnurri binding sites within the reporter fragment led to expression in most hub cells (Fig. 1C). Collectively, our data suggest strongly that *magu* is expressed from hub cells, but potentially not from all hub cells equally.

*magu* encodes a putative matricellular protein, which is defined as a secreted protein that could regulate cell-matrix interactions. To investigate the localization of Magu, we raised antibodies against an N-terminal portion of Magu. Sera from immunized rabbits showed specific immunoreactivity on western blots to bacterially expressed, His-tagged Magu protein (data not shown). After preabsorption using wildtype testes (see Materials and Methods), we observed an enriched pattern of puncta in the hub region (Fig.1D, D'). Magu accumulated along the interfaces among hub cells (Fig.1D upper inset), similar to FascIII. In addition, it was present along the interface between hub cells and stem cells (Fig.1D lower inset, arrowheads). Since this serum was effective only sporadically, we also explored the accumulation of Magu by using a second antibody, raised against a C-terminal peptide (Vuilleumier et al., 2010). This antiserum reproducibly exhibited an extended distribution of Magu relative to the hub, with strongly staining puncta appearing among stem cells and their daughters (Fig. 1E, and insets; E', bracket). In addition, there was a more subtle enrichment in a ring along the hub cell-stem cell interface (Fig. 1E lower inset and E', arrowhead), reminiscent of that obtained with the N-terminal antisera. These patterns were reduced significantly in testes bearing mutations in *magu* (Fig. 1F, F'). Since Magu is predicted to be a secreted protein, we attempted to visualize Magu under conditions where the antibody could only detect extracellular proteins (see Materials and Methods). Using the C-terminal antiserum (but not the N-terminal antiserum) a strong punctuate signal was observed only in optical sections above the hub (Fig. 1G), and this pattern disappeared in the *magu* mutant (Fig. 1H). We do not know if the differences in accumulation pattern comparing the two antisera reflect differing distributions or availabilities of their respective epitopes. Nevertheless, these data are consistent with the model whereby *magu* is transcribed in hub cells, and its encoded protein secreted and accumulates in the vicinity of neighboring cells.

## Generating *magu* mutants

In order to investigate the function of *magu*, we identified mutations among transposon insertion lines and generated null mutations by manipulating those lines (see Materials and Methods). Two insertions, KG02847b (KG) and d00269, were homozygous viable and exhibited no detectable phenotype. These insertions were mapped upstream of exon 3 of *magu* (Fig.2A). However, flies homozygous for the insertion e00439, or heteroallelic combinations of e00439 and f02256 were viable and exhibited both a wing vein defect (Supplemental Fig.1B, C) and a testis phenotype (see below). These PiggyBac insertions each mapped near the 3' end of exon 3 (Fig.2). To obtain potentially stronger mutant alleles, we generated deletions encompassing some or all of the genomic region containing *magu*. Deletion mutant I lacked exon 3, which contained the *magu* translational start codon (Fig.2).

More extensive deletions were generated from the KG insertion. Individual deletions removed the whole *magu* region downstream of KG, and extended from 15 to 374 kilobases downstream of *magu* (Fig.2). By comparing the strength of both the wing vein and testis phenotypes, we established that e00439 and deletion I behave as null alleles of *magu*, while f02256 is a strong loss-of-function allele.

## Magu is required for maintenance of GSCs

Compared with wildtype, *magu* mutant testes appeared thinner, containing fewer germ cells (data not shown). Since *magu* was expressed from hub cells, we tested whether a GSC defect might account for this phenotype. We scored GSCs by counting individual small-size germ cells attached to the hub. In one mutant condition, $magu^{e00439}/magu^{f02256}$, the median GSC number per testis was only 3, whereas the sibling control carried a median of 8 GSCs (Fig.3A, B; Table 1). Moreover, *magu* mutant testes displayed germ cells with branched fusomes next to the hub (Fig.3D arrowhead), indicating they were differentiating and no longer *bona fide* stem cells. We found a similarly dramatic reduction in the median number of GSCs for other *magu* mutant combinations (Table 1). We also noticed that there was variation in phenotypic strength. For a given allele, or allele combination, some mutant testes were devoid of all GSCs, while others retained some GSCs. As a measure of this, we also calculated the percentage of testes with GSCs for each genotype. That fraction depended on the genotype and growth condition used in a particular experiment (Table 1).

We took two approaches to confirm that the defect in GSC maintenance indeed resulted from mutation of *magu*. First, the transposon insertion, e00439, was remobilized to establish a revertant line. We found that GSCs were substantially restored in flies carrying this revertant chromosome placed over the f02256 mutant (Table 1). While there remained a slight difference in the median number of GSCs retained in the revertants compared to controls, all revertant testes now retained GSCs. Second, we attempted to rescue the GSC defect by restoring *magu* expression in the mutant background. To accomplish this, we used the hub cell driver *upd*-Gal4 to express *magu* containing either an N-terminal (V5) (Vuilleumier et al., 2010) or C-terminal (Myc) epitope tag. To promote continued and robust expression using the Gal4-UAS system, young adults were aged at 29°C for either 3 days or 12 days before analysis. We scored both median GSC number, and the fraction of testes maintaining GSCs. Using both measures, we obtained statistically significant, but incomplete rescue. Among mutant siblings from these crosses, it was common that more than half of the testes contained no GSCs. When either N-terminal V5- or C-terminal Myc-tagged *magu* was expressed in the mutants, the fraction of testes with GSCs increased to more than 50%, and sometimes approached or equaled 100% (Table 1) Restoration of V5-*magu* also increased the median number of GSCs for both younger and older flies (Table 1). But restoration of *magu*-Myc only led to an increase in median GSC number for older flies (Fig.3E; Table 1). This was the case using several different UAS-*magu*-Myc or GFP transgenic insertion lines (data not shown). Thus, the slightly different behavior of N-terminal versus C-terminal rescuing construct might be due to a difference in inherent activity of the proteins produced. We observed a similar difference in rescuing ability for the wing vein defect of *magu* mutants (Supplemental Fig.1D, E). In spite of the difference in transgene effectiveness, collectively, the data demonstrate that Magu is required for normal GSC number in the adult testis. The loss of GSCs was also observed in *magu* mutant gonads from the 3rd instar larvae (Table 1). But the phenotype in gonads was much less severe than in adult testes, because the median GSC number per mutant gonad was much higher, and all mutant gonads still retained some GSCs (Table 1). Thus we conclude Magu affects male GSC maintenance.

## Magu does not affect CySC or hub cell number

In the normal testis, GSC self-renewal depends on CySCs and hub cells (Leatherman and DiNardo, 2008; Leatherman and DiNardo, 2010). Thus the loss of GSCs that we observed in *magu* mutant testes could be a secondary effect attributed to either CySCs or hub cells. To determine whether there are any defects among CySCs in the *magu* mutants, we analyzed the number of CySCs by staining for Zfh1, an essential CySC marker (Leatherman and DiNardo, 2008). In contrast to the GSCs, significant numbers of Zfh1-expressing cells were still present in the mutant (Fig.4B; Table 2). These cells were arranged more compactly around the hub, presumably because they now occupied the space vacated by the loss of GSCs (Fig.4A, B). To investigate whether CySCs in the mutants function properly, we marked cycling cells by S phase labeling using Edu. The ratio of Edu and Zfh1 double positive cell number to Zfh1 single positive cell number in the mutants was indistinguishable from that in the sibling controls (Fig.4C, D arrowhead; Table 2), indicating that the mutant CySCs cycle properly. To further confirm the undifferentiated state of CySCs in mutant testes, we examined Eya expression as a marker for cyst cell differentiation (Supplemental Fig.2). The small-sized cyst cells close to hub did not express Eya (Supplemental Fig.2B, B'). We occasionally noted some Eya positive cyst cells near the hub in *magu* mutants (Supplemental Fig. 2C arrowhead, C'). But these cells were much larger, suggesting they were late-stage cyst cells, associated with spermatocytes, that had failed to be pushed away from the hub due to the reduced production of germ cells. Thus, taken together with their expression of Zfh1 and cell cycling behavior, we conclude that these cells were *bona fide* CySCs.

To test whether Magu affects the maintenance of the hub, we counted hub cell numbers using the cell biological hub marker FascIII (Fig.4E, F). We found *magu* mutants contained a similar number of hub cells compared to sibling controls (Table 2). To determine whether these hub cells were capable of functioning properly, we asked whether they expressed a key niche signal, *upd*. Indeed, *upd* was expressed normally in *magu* mutant testes, and there was no difference in the number of *upd* positive hub cells comparing mutants and sibling controls (Fig.4G, H; Table 2). Thus we conclude that the loss of GSCs in *magu* mutants is not secondary to depletion or defect of either of the essential niche cell types, the CySCs or hub cells.

## Magu affects GSC maintenance through the BMP signaling pathway

It has been shown that JAK-STAT signaling is important for the establishment and maintenance of GSCs (Kiger et al., 2001; Sheng et al., 2009; Tulina and Matunis, 2001). As shown in Fig.4H, *magu* mutants did not affect the expression of Upd, a key JAK/STAT-activating ligand expressed from hub cells. To test whether *magu* mutants affect activation of the STAT pathway, we analyzed the accumulation of STAT protein (Chen et al., 2002). In control testes, STAT accumulated among the first tier of cells surrounding the hub (Fig. 5A). This represented STAT accumulation in both nearby germ cells and somatic cells (the GSCs and CySCs). In *magu* mutants, which have a normal complement of CySCs and occasionally have some remaining GSCs, STAT accumulated in cells surrounding the hub in a similar pattern to wildtype (Fig.5B). Therefore Magu does not appear to affect STAT pathway activation.

The second signaling pathway that is required for GSC maintenance is BMP (Kawase et al., 2004; Leatherman and DiNardo, 2010; Schulz et al., 2004; Shivdasani and Ingham, 2003). To test whether Magu affects this pathway, we examined the activation of Mad, a transducer of BMP signaling. In several tissues, the accumulation of phosphorylated Mad (pMad) can be used as a read-out of BMP pathway activation. We never observed pMad staining among germ cells surrounding the hub in *magu* mutant testes (Fig. 5D). However, we could not

conclude that BMP pathway activation was compromised because we found it difficult to observe pMad staining consistently in the GSCs of control and wildtype testes. In our hands, only occasionally would control testes present with pMad accumulation among the tier of germ cells surrounding the hub (Fig.5C). In contrast to that inconsistency in testes, gonads from 3rd instar larvae reproducibly showed pMad staining (Fig.5E). In gonads from *magu* mutants, we never observed pMad accumulation in germ cells surrounding the hub (Fig. 5F), suggesting strongly that BMP pathway activation was compromised in *magu* mutants. In passing, we noted two characteristics of pMad accumulation in control larval gonads. First, in some gonads, not all the GSCs were positive (data not shown). Second, we often observed pMad accumulation in the second tier germ cells (Fig 5E, arrowheads), likely gonialblast progeny of the GSCs. This suggests occasional, more broad BMP pathway activation than previously reported.

To confirm the apparent diminution of BMP signaling in *magu* mutants, we examined a presumed target of BMP activation, the *bam* gene, whose expression is repressed in BMP-signaled cells. We used a *bam* promoter-GFP transgene (*bam*-GFP) (Chen and McKearin, 2003) as a read-out for pMad activity. In control testes, *bam*-GFP was expressed only in amplifying gonial cells, as expected (Fig.5G; 9 testes analyzed). In mutant testes, of 18 testes analyzed, only 5 had residual GSCs, and in all of them there were GSCs that exhibited *bam*-GFP (Fig.5H, arrowhead). This data supports the hypothesis that Magu affects BMP signaling.

If *magu* was indeed required for proper BMP activation in germ cells, constitutive activation of the BMP pathway in the germline could bypass the requirement for *magu*. To accomplish this, we expressed an activated form of BMP type I receptor Thickvein (TkvA) using the germ cell driver, *nanos*-Gal4:VP16. Indeed, this raised the fraction of testes with GSCs from 63% to 100% (Table 1). The median GSC number also doubled compared to that observed in mutants (Fig.5I; Table 1). Thus intrinsic activation of the BMP pathway in germ cells can bypass the need for *magu*. This result is consistent with a simple model that GSCs are lost because BMP activation is compromised in *magu* mutants.

*magu* encodes a secreted protein, expressed selectively from hub cells, and accumulating among cells nearby. Our data suggests that Magu is necessary for proper BMP activation within adjacent germ cells. BMP ligands appear to be produced by both hub cells and CySCs, but not by germ cells (Kawase et al., 2004; Shivdasani and Ingham, 2003). To test whether *magu* is required for BMP ligand production in the hub cells, we attempted to rescue the GSC defect using the germ cell driver *nanos*-Gal4:VP16. Indeed, we observed a statistically significant increase in median GSC number in such testes (Fig.3F; Table 1). This suggests that BMP ligands are produced normally in *magu* mutants, and Magu is downstream of ligand production. This also suggests that Magu likely acts cell-nonautonomously in the extracellular environment.

## Discussion

Here, by following up on a previous microarray approach that identified transcripts enriched at the testis tip, we show that *magu* plays an important role in GSC maintenance. We also provide strong evidence that it does so by modulating BMP activation in germ cells. *magu* encodes a secreted protein of the SPARC/BM-40/osteonectin family, recently shown to ensure the proper activity gradient for the BMP morphogen, Dpp, across the developing wing epithelium (Vuilleumier et al., 2010). The role we have characterized for Magu in the testis niche exhibits some similarities as well as differences to that proposed for the wing.

## Magu serves as a BMP modulator to maintain GSCs in the testis

It has been shown that the BMP pathway is activated and required in GSCs, whereas the JAK-STAT pathway is activated and required in both GSCs and CySCs (Issigonis et al., 2009; Kawase et al., 2004; Kiger et al., 2001; Leatherman and DiNardo, 2010; Schulz et al., 2004; Shivdasani and Ingham, 2003; Tulina and Matunis, 2001). Our data shows that *magu* is required for maintenance of GSCs, but not CySCs, and that BMP activation was impaired in germ cells adjacent to the hub in *magu* mutants. We also found that forcing activation of the BMP pathway in germ cells substantively rescued the *magu* phenotype. Thus, we conclude that the primary role of *magu* in the testis niche is to modulate BMP signaling and thereby maintain GSCs.

Superficially, our results suggest that Magu works in a manner similar to that described in the wing epithelium, where Magu facilitates the transport of BMP ligands to establish the proper signaling gradient. However, there are several differences comparing the wing with the testis niche.

The most obvious is that to control wing patterning, BMP signaling is graded and must be effective over a long range. Thus, Dpp is expressed from a stripe of cells in the center of the wing disc, while the region where BMP activation is modulated by Magu is located far laterally, many tens of cells away from the ligand source (Vuilleumier et al., 2010). In striking contrast to this situation, BMP ligands are produced in hub cells and CySCs of testes, which are directly adjacent to GSCs, where pathway activation is required (Kawase et al., 2004; Shivdasani and Ingham, 2003). In the testis, there is no documented graded requirement, and, if anything, it is likely that pathway activation must be restricted to cells near the niche to ensure that few cells take on stem cell character. Therefore, while Magu is thought to assist the movement of Dpp over a long range in the wing (Vuilleumier et al., 2010), there is no need for long-range transport for GSC maintenance in the testis. This distinction between the two systems suggests that key mechanistic differences remain to be uncovered for how Magu affects BMP signaling.

One way that Magu supports robust signaling far from the BMP ligand source in the wing is that *magu* gene expression is engaged by a feedback circuit in order to be used as a positive modulator of signaling. Thus, *magu* expression is repressed in areas of relatively high signaling, and that repression is relieved in regions of low signaling. Its action in the low signaling region is to promote signaling even though these areas are far from the ligand source (Vuilleumier et al., 2010). In fact, expressing *magu* ectopically in the area of high signaling serves to dampen signaling there, while enhances signal at a distance, presumably by promoting movement or stabilization of the ligand. In the testis niche, we do have some evidence for feedback regulation, as a reporter construct mutated for pMad/Medea/Schnurri complex binding sites (Vuilleumier et al., 2010) is expressed more robustly, and in more hub cells. However, in contrast to the wing, we have no evidence that this negative feedback regulation is necessary in the testis niche, as overexpression of *magu* had no discernable effect on GSC numbers (data not shown).

One other potential difference between the wing and testis niche is that the BMP ligands acted on by Magu might differ in the two systems. Vuilleumier et al. have addressed the function of Magu with respect to Dpp, the principal BMP ligand used globally for wing patterning. However, the major BMP ligand for male GSC maintenance appears to be Gbb (Kawase et al., 2004; Shivdasani and Ingham, 2003). This difference could have consequences for the mechanism by which Magu influences BMP signaling comparing the two systems. For example, although Dpp does not interact directly with Magu (Vuilleumier et al., 2010), the potential remains that Magu might bind to Gbb for GSC maintenance.

In this regard, it is worth noting that *gbb* is expressed throughout the wing (Khalsa et al., 1998), and that compromising *gbb* function does generate a wing vein phenotype similar to *magu* mutants (Bangi and Wharton, 2006; Ray and Wharton, 2001). Thus, in the wing, even though the focus has been on Dpp, perhaps there is an effect also on Gbb transport and/or signaling. Thus, further investigation of the modulation of BMP signaling by Magu in both the wing and testis niche should be revealing.

### How might Magu modulate BMP signaling in the testis niche?

The fact that overexpressing a constitutively active form of BMP type I receptor in the germline can rescue the GSC phenotype suggests that Magu acts upstream of receptor binding. This is in agreement with its proposed role in the wing and also preliminary analysis in zebrafish (Vuilleumier et al., 2010). There are a number of membrane-associated and secreted factors that Magu might influence to modulate BMP signaling.

In the wing, Magu interacts directly with Dally, a HSPG (heparan sulfate proteoglycan) (Vuilleumier et al., 2010). Interestingly, Dally and its homologue Dally-like (Dlp) are also important for male GSC maintenance (Guo and Wang, 2009; Hayashi et al., 2009). While we have not found genetic interactions between *magu* and *dally*, *dlp* or several other genes needed for HSPG biosynthesis, some preliminary data indicate that overexpressing *dlp* in the germ cells can increase the fraction of testes retaining GSCs among *magu* mutants (data not shown). Dlp has been shown to be enriched among hub cells (Hayashi et al., 2009), but we have had no success in reproducing this suggestive distribution (Q.Z. and S.D., unpublished results). Therefore, further experiments are needed to test for interactions between Magu and Dlp or other HSPGs in GSC maintenance.

Given that Magu is secreted from hub cells, its localization could have suggested a more specific hypothesis for its action in the testis niche. However, *magu* protein localization among cells of the niche appears complex. An antibody we raised against an N-terminal portion of Magu exhibits punctate signal restricted among hub cells, and at the hub-GSC interface, but this serum was effective only sporadically. A second serum directed against a C-terminal peptide (Vuilleumier et al., 2010) robustly exhibits the same punctate pattern among hub cells, but also reveals a slightly extended distribution among stem cells and their daughters near the hub. Additionally, this serum revealed strong punctate signal likely among the extracellular matrix (ECM) near the hub. It is not possible at this time to distinguish whether the pool of Magu associated with ECM or the more generally distributed pool is active for GSC maintenance.

However, considering the close proximity of hub cells to GSCs, it is simplest to envision that Magu acts along the hub cell-germline stem cell interface, where the interaction of BMP ligands and receptors occurs. It is possible that Magu facilitates interactions between BMPs and their receptors via formation of ternary ligand/Magu/receptor complexes. This model has been shown for Crossveinless 2 (Cv2), an extracellular BMP modulator engaged for crossvein patterning in the wing (Serpe et al., 2008). Cv2 can also bind to Dally, and the Cv2-HSPG interaction is likely important for normal BMP signaling in crossvein patterning (Serpe et al., 2008). Magu and its vertebrate orthologues SMOC1/2 have two Thyroglobulin type-1 repeats. It has been shown that proteins with such repeats can inhibit extracellular proteases (Mihelic and Turk, 2007). Thus, although Cv2 appears to have no effect on the function of Tolkin, the protease promoting BMP signaling in crossvein patterning (Serpe et al., 2008), it is reasonable to speculate that Magu may function as a protease inhibitor to protect BMP ligands from being degraded by extracellular proteases.

Alternatively, the enrichment we observed among the ECM is interesting. Among the family of proteins to which Magu belongs, SPARC interacts with type IV Collagen, a component of

basement membranes (Brekken and Sage, 2001), and SMOC1/2 are associated with basement membranes (Vannahme et al., 2003; Vannahme et al., 2002). Interestingly, Viking (Vkg), the type IV collagen in *Drosophila*, is involved in the female GSC maintenance, potentially by sequestration of Dpp, thereby restricting BMP signaling in the germarium (Wang et al., 2008). It would be interesting to investigate whether Vkg also plays a similar role in the testis, and interacts with Magu to maintain a normal number of GSCs.

### Highlights

➤ We study how niche signals maintain stem cells

➤ *magu* encodes an extracellular matrix protein expressed from niche cells

➤ *magu* is specifically and directly required to maintain germline stem cells

➤ Magu is an extracellular BMP modulator in the testis niche.

## Supplementary Material

Refer to Web version on PubMed Central for supplementary material.

## Acknowledgments

## References

Bangi E, Wharton K. Dpp and Gbb exhibit different effective ranges in the establishment of the BMP activity gradient critical for Drosophila wing patterning. Developmental biology. 2006; 295:178–193. [PubMed: 16643887]

Brekken RA, Sage EH. SPARC, a matricellular protein: at the crossroads of cell-matrix communication. Matrix Biol. 2001; 19:815–827.

Chen D, McKearin DM. A discrete transcriptional silencer in the bam gene determines asymmetric division of the Drosophila germline stem cell. Development. 2003; 130:1159–1170. [PubMed: 12571107]

Chen H-W, Chen X, Oh S-W, Marinissen MJ, Gutkind JS, Hou SX. mom identifies a receptor for the Drosophila JAK/STAT signal transduction pathway and encodes a protein distantly related to the mammalian cytokine receptor family. Genes & development. 2002; 16:388–398. [PubMed: 11825879]

Cheng J, Tiyaboonchai A, Yamashita YM, Hunt AJ. Asymmetric division of cyst stem cells in Drosophila testis is ensured by anaphase spindle repositioning. Development. 2011; 138:831–837. [PubMed: 21303845]

Fabrizio JJ, Boyle M, DiNardo S. A somatic role for eyes absent (eya) and sine oculis (so) in Drosophila spermatocyte development. Developmental biology. 2003; 258:117–128. [PubMed: 12781687]

Fuller MT, Spradling AC. Male and female Drosophila germline stem cells: two versions of immortality. Science (New York, N.Y.). 2007; 316:402–404.

Guo Z, Wang Z. The glypican Dally is required in the niche for the maintenance of germline stem cells and short-range BMP signaling in the Drosophila ovary. Development (Cambridge, England). 2009; 136:3627–3635.

Hardy RW, Tokuyasu KT, Lindsley DL, Garavito M. The germinal proliferation center in the testis of Drosophila melanogaster. Journal of Ultrastructure Research. 1979; 69:180–190. [PubMed: 114676]

Hayashi Y, Kobayashi S, Nakato H. Drosophila glypicans regulate the germline stem cell niche. The Journal of cell biology. 2009; 187:473–480. [PubMed: 19948496]

Issigonis M, Tulina N, de Cuevas M, Brawley C, Sandler L, Matunis E. JAK-STAT signal inhibition regulates competition in the Drosophila testis stem cell niche. Science. 2009; 326:153–156. [PubMed: 19797664]

Kawase E, Wong MD, Ding BC, Xie T. Gbb/Bmp signaling is essential for maintaining germline stem cells and for repressing bam transcription in the Drosophila testis. Development (Cambridge, England). 2004; 131:1365–1375.

Khalsa O, Yoon JW, Torres-Schumann S, Wharton Ka. TGF-beta/BMP superfamily members, Gbb-60A and Dpp, cooperate to provide pattern information and establish cell identity in the Drosophila wing. Development (Cambridge, England). 1998; 125:2723–2734.

Kiger, aa; Jones, DL.; Schulz, C.; Rogers, MB.; Fuller, MT. Stem cell self-renewal specified by JAK-STAT activation in response to a support cell cue. Science (New York, N.Y.). 2001; 294:2542–2545.

Leatherman JL, DiNardo S. Zfh-1 controls somatic stem cell self-renewal in the Drosophila testis and nonautonomously influences germline stem cell self-renewal. Cell stem cell. 2008; 3:44–54. [PubMed: 18593558]

Leatherman JL, DiNardo S. Germline self-renewal requires cyst stem cells and stat regulates niche adhesion in Drosophila testes. Nat Cell Biol. 2010; 12:806–811. [PubMed: 20622868]

Li L, Xie T. Stem cell niche: structure and function. Annual review of cell and developmental biology. 2005; 21:605–631.

Li Y, Tower J. Adult-specific over-expression of the Drosophila genes magu and hebe increases life span and modulates late-age female fecundity. Molecular genetics and genomics : MGG. 2009; 281:147–162. [PubMed: 19011900]

Matunis E, Tran J, Gönczy P, Caldwell K, DiNardo S. Punt and Schnurri Regulate a Somatically Derived Signal That Restricts Proliferation of Committed Progenitors in the Germline. Development (Cambridge, England). 1997; 124:4383–4391.

Mihelic M, Turk D. Two decades of thyroglobulin type-1 domain research. Biological chemistry. 2007; 388:1123–1130. [PubMed: 17976004]

Parks AL, Cook KR, Belvin M, Dompe Na, Fawcett R, Huppert K, Tan LR, Winter CG, Bogart KP, Deal JE, Deal-Herr ME, Grant D, Marcinko M, Miyazaki WY, Robertson S, Shaw KJ, Tabios M, Vysotskaia V, Zhao L, Andrade RS, Edgar Ka, Howie E, Killpack K, Milash B, Norton A, Thao D, Whittaker K, Winner Ma, Friedman L, Margolis J, Singer Ma, Kopczynski C, Curtis D, Kaufman TC, Plowman GD, Duyk G, Francis-Lang HL. Systematic generation of high-resolution deletion coverage of the Drosophila melanogaster genome. Nature genetics. 2004; 36:288–292. [PubMed: 14981519]

Ray RP, Wharton Ka. Context-dependent relationships between the BMPs gbb and dpp during development of the Drosophila wing imaginal disk. Development (Cambridge, England). 2001; 128:3913–3925.

Schulz C, Kiger Aa, Tazuke SI, Yamashita YM, Pantalena-Filho LC, Jones DL, Wood CG, Fuller MT. A misexpression screen reveals effects of bag-of-marbles and TGF beta class signaling on the Drosophila male germ-line stem cell lineage. Genetics. 2004; 167:707–723. [PubMed: 15238523]

Serpe M, Umulis D, Ralston A, Chen J, Olson DJ, Avanesov A, Othmer H, O'Connor MB, Blair SS. The BMP-binding protein Crossveinless 2 is a short-range, concentration-dependent, biphasic modulator of BMP signaling in Drosophila. Developmental cell. 2008; 14:940–953. [PubMed: 18539121]

Sheng XR, Posenau T, Gumulak-Smith JJ, Matunis E, Van Doren M, Wawersik M. Jak-STAT regulation of male germline stem cell establishment during Drosophila embryogenesis. Developmental biology. 2009; 334:335–344. [PubMed: 19643104]

Shivdasani, Aa; Ingham, PW. Regulation of Stem Cell Maintenance and Transit Amplifying Cell Proliferation by TGF-β Signaling in Drosophila Spermatogenesis. Current Biology. 2003; 13:2065–2072. [PubMed: 14653996]

Terry, Na; Tulina, N.; Matunis, E.; DiNardo, S. Novel regulators revealed by profiling Drosophila testis stem cells within their niche. Developmental biology. 2006; 294:246–257. [PubMed: 16616121]

Tulina N, Matunis E. Control of stem cell self-renewal in Drosophila spermatogenesis by JAK-STAT signaling. Science (New York, N.Y.). 2001; 294:2546–2549.

Vannahme C, Gösling S, Paulsson M, Maurer P, Hartmann U. Characterization of SMOC-2, a modular extracellular calcium-binding protein. The Biochemical journal. 2003; 373:805–814. [PubMed: 12741954]

Vannahme C, Smyth N, Miosge N, Gösling S, Frie C, Paulsson M, Maurer P, Hartmann U. Characterization of SMOC-1, a novel modular calcium-binding protein in basement membranes. The Journal of biological chemistry. 2002; 277:37977–37986. [PubMed: 12130637]

Vuilleumier R, Springhorn A, Patterson L, Koidl S, Hammerschmidt M, Affolter M, Pyrowolakis G. Control of Dpp morphogen signalling by a secreted feedback regulator. Nature cell biology. 2010; 12:611–617.

Wang X, Harris RE, Bayston LJ, Ashe HL. Type IV collagens regulate BMP signalling in Drosophila. Nature. 2008; 455:72–77. [PubMed: 18701888]

Yamashita YM, Jones DL, Fuller MT. Orientation of asymmetric stem cell division by the APC tumor suppressor and centrosome. Science (New York, N.Y.). 2003; 301:1547–1550.
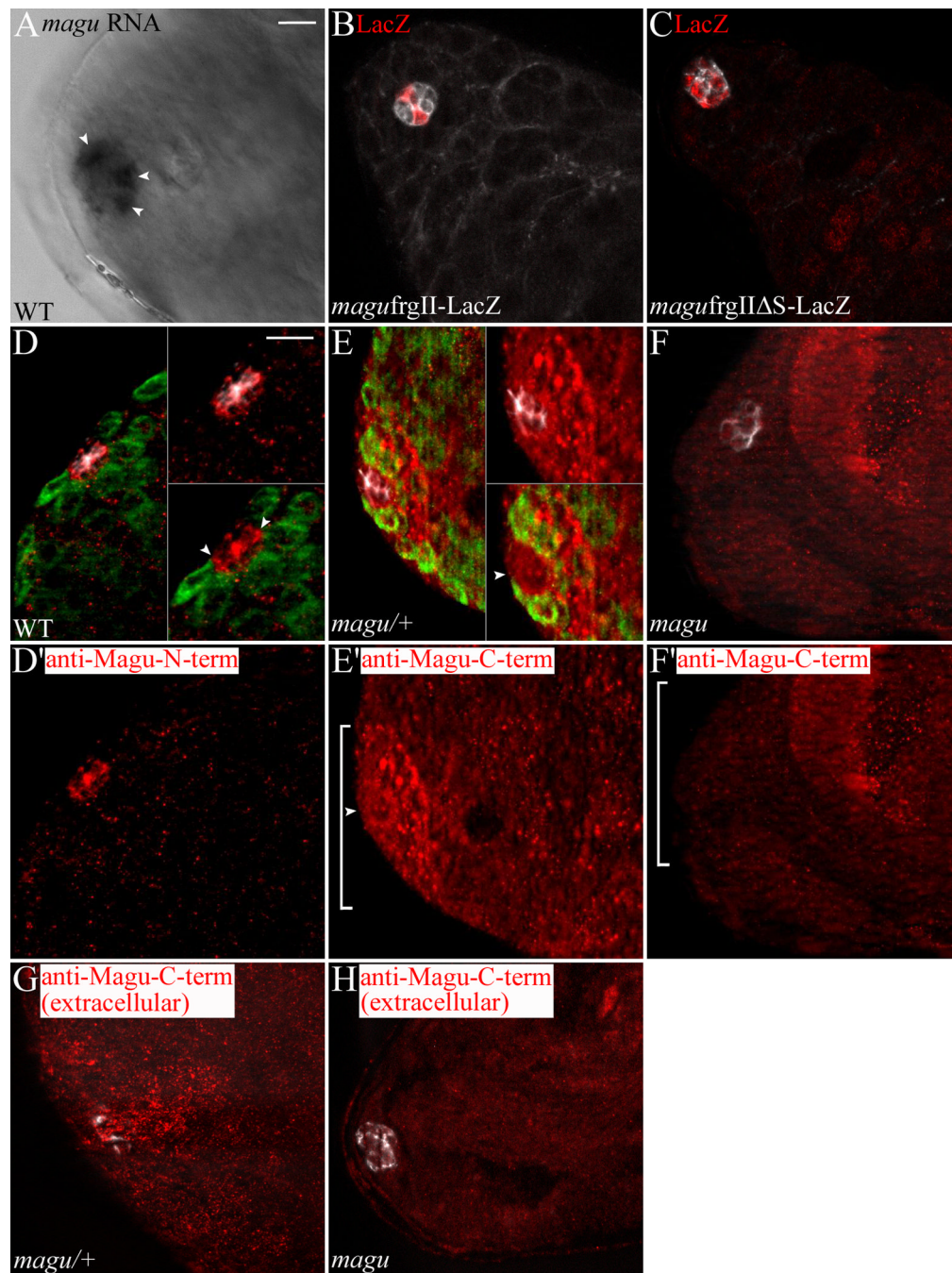
**Figure 1.**
*magu* is expressed from hub cells. **(A)** *In situ* hybridization in wildtype testes (WT; *w1118*) revealing *magu* RNA among hub cells. Sometimes *magu* was not expressed equivalently in all hub cells. The testis shown here exhibited enriched *magu* RNA in three hub cells (arrowheads). **(B)** *magu* reporter line frgII-lacZ [Vuilleumier et al., 2010]: LacZ (red) accumulates in a few hub cells (E-Cadherin, white). Of 15 testes analyzed, 3 exhibited no hub expression, whereas the remaining 12 testes contained 1 or 2 LacZ positive hub cells. **(C)** *magu* reporter line frgIIΔS-lacZ, wherein Mad/Medea/Schnurri binding sites were mutated: in 8 of 10 testes analyzed, LacZ (red) now accumulated in most hub cells (white).

This suggests that the BMP pathway is active in hub cells. There is also LacZ accumulation in late-stage spermatogonia. We do not know if this reflects some latent regulation of *magu* in those cells. **(D)** Anti-Magu-N-term on WT testes: this serum sporadically exhibited an enhanced, punctate signal (red) at the hub (FascIII, white). **(D')** Anti-Magu-N-term channel alone. Accumulation was observed along the interfaces between hub cells (D, upper inset), and along the hub cell-germ cell interface (D, lower inset, arrowheads; Vasa labeled germ cells, green). **(E)** Anti-Magu-C-term [Vuilleumier et al., 2010] on *magu*/+ (magudeletionI/ *CyOkr-Gal4UAS-GFP*) testes: this serum routinely revealed a broader domain of Magu accumulation (red) in the area surrounding the hub (white). **(E')** Anti-Magu-C-term channel alone. The signal appeared as an accumulation of quite large puncta adjacent to the hub (E, upper inset), located approximately as far as the second tier of germ cells (E, lower inset). Accumulation along the interface between hub and germ cells was detectable, but was less punctate than for the anti-Magu-N-term antibody (E lower inset and E', arrowhead). **(F)** Anti-Magu-C-term on *magu*$^{deletionI}$/*magu*$^{deletionI}$ testes: accumulation (red) surrounding the hub (white) was significantly reduced. **(F')** Anti-Magu-C-term channel alone. We noted that in mutants small puncta remained, as well as puncta in nuclei of late stage spermatogonia and cyst cells (data not shown). This must be due to cross-reaction with non-Magu epitopes. **(G)** Staining *magu*/+ testes with the anti-Magu-C-term sera (red) at 4°C, prior to fixation and using no detergent (see Materials and Methods) revealed an extracellular Magu accumulation, visible in sections above the hub region (FascIII, white). **(H)** The extracellular, punctate signal disappeared (red) in *magu*$^{deletionI}$/*magu*$^{deletionI}$ testes. Scale bar: 10 μm.
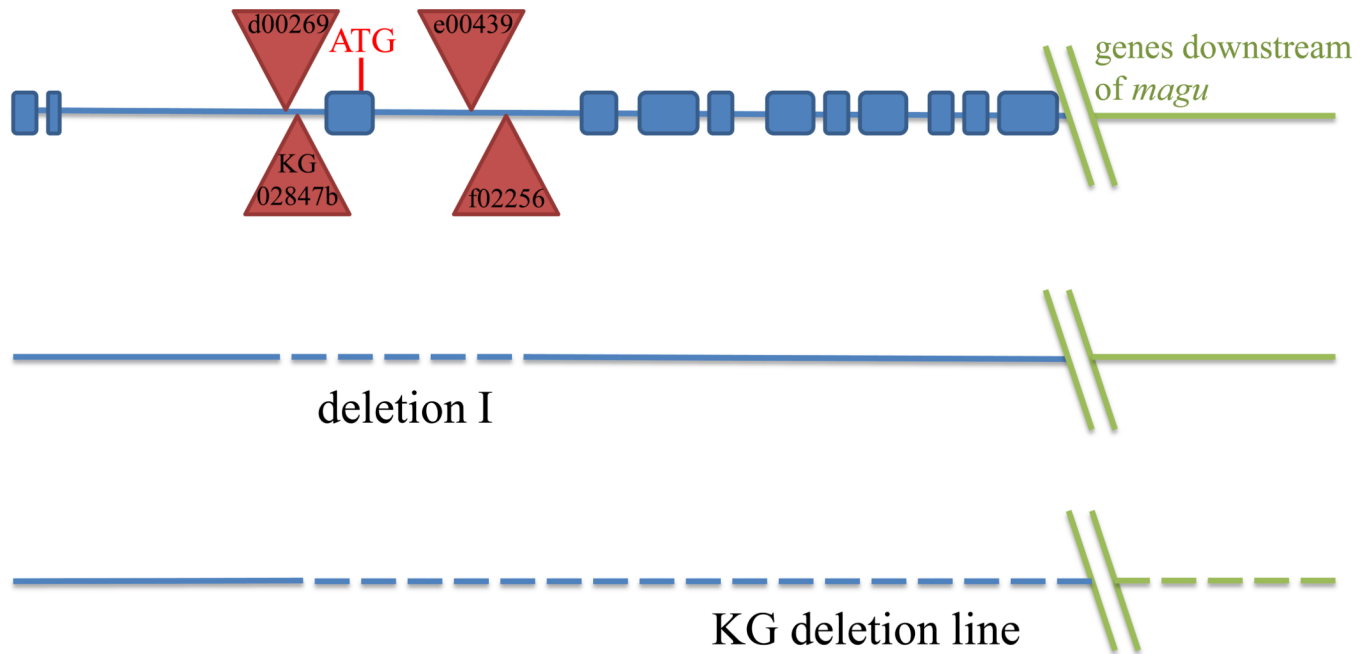
**Figure 2.**
*magu* gene structure and mutants. The genomic region in the vicinity of *magu* (not to scale), with its exons in blue. Insertion elements used to create deletion mutants are denoted by red triangles. Genomic sequences deleted in mutants described here are indicated by dashed lines. Deletion I (dashed line) lacks the sequence between the PiggyBac insertions d00269 and f02256, and thus deletes exon 3, which contains the translational start codon and signal sequence. Extent of deletions in KG deletion lines (see Materials and Methods) begins from KG02847b to at least 15 kilobases downstream of *magu*.
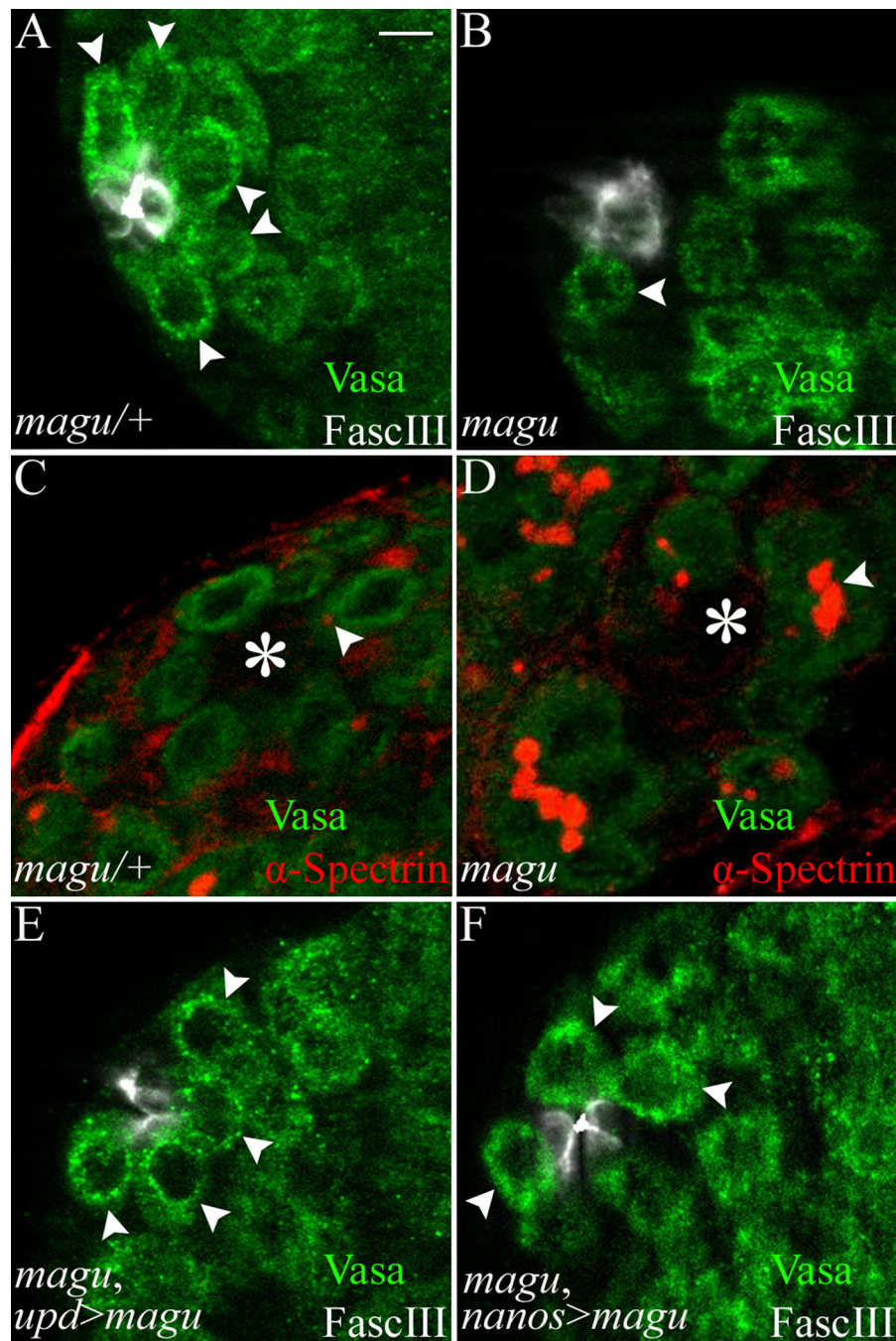
**Figure 3.**
GSCs are lost in *magu* mutants. **(A)** *magu*/+ (*magu*<sup>e00439 or f02256</sup>/*CyOkr-Gal4UAS-GFP*). A single focal section exhibited five GSCs (arrowheads; Vasa labeled germ cells, green) attached to the hub (FascIII, white). **(B)** *magu*<sup>e00439</sup>/*magu*<sup>f02256</sup>. A representative single focal section showed one remaining GSC (arrowhead). **(C)** *magu*/+. Anti-α-Spectrin revealed a dot fusome (red, arrowhead) marking a GSC adjacent to the hub (asterisk). Other GSCs contain dot fusomes in other focal planes. **(D)** *magu*<sup>e00439</sup>/*magu*<sup>f02256</sup>. In mutants, germ cell clusters exhibiting a branched fusome (red, arrowhead) could be observed adjacent to the hub (asterisk). This is indicative of differentiation away from the stem cell state. **(E)**

*upd*-Gal4; *magu*^e00439/magu^f02256^; UAS-*magu*-Myc. **(F)** *magu*^e00439/magu^f02256^; *nanos*-Gal4/UAS-*magu*-Myc. In *magu* mutants, restoration of *magu* to hub cells (E) or providing *magu* from an ectopic site (from germline cells, F) resulted in the retention of GSCs (arrowheads). Scale bar: 5 μm.
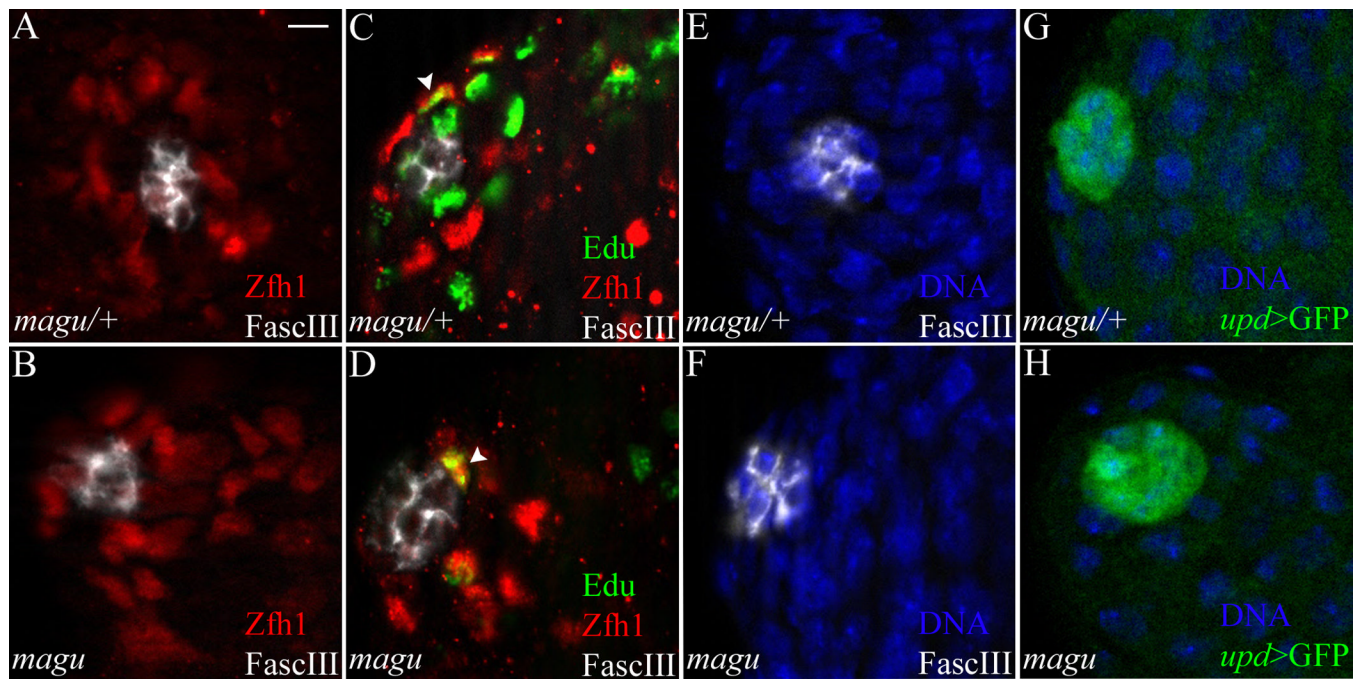
**Figure 4.**
CySCs and hub cells are maintained in *magu* mutants. **(A)** *magu*/+ (*magu*$^{e00439 \text{ or } f02256}$/*CyOkr-Gal4UAS-GFP*). Zfh1-expressing CySCs (red) surrounded the hub (white). **(B)** *magu*$^{e00439}$/*magu*$^{f02256}$. A similar number of Zfh1-expressing CySCs (red) was observed in mutant testes. **(C)** *magu*/+. A testis was pulse-labeled with EdU (green) to determine the S-phase index of CySCs (Zfh1, red) surrounding the hub (white). The arrowhead marked one such CySC in S-phase. EdU+ nuclei that were Zfh1− were germ cells in S-phase. **(D)** *magu*$^{e00439}$/*magu*$^{f02256}$. Cycling CySCs were also observed in mutant testes; one is shown here (arrowhead). **(E)** *magu*/+. Hub cells were outlined and scored by FascIII accumulation (white; Hoechst labeled nuclei, blue). **(F)** *magu*$^{e00439}$/*magu*$^{f02256}$. The hub in mutant testes appeared normal, and contained a normal number of FascIII+ cells. **(G)** *magu*/+ (*upd*-Gal4 UAS-GFP;*magu*$^{e00439 \text{ or } f02256}$/*CyOkr-Gal4UAS-GFP*). Hub cells expressed *upd*, as revealed by *upd*>GFP (green). **(H)** *upd*-Gal4 UAS-GFP;*magu*$^{e00439}$/*magu*$^{f02256}$. A normal number of *upd*-expressing cells was observed for hubs from mutant testes. See Table2 for quantitation of data from all panels. Scale bar: 5 μm.
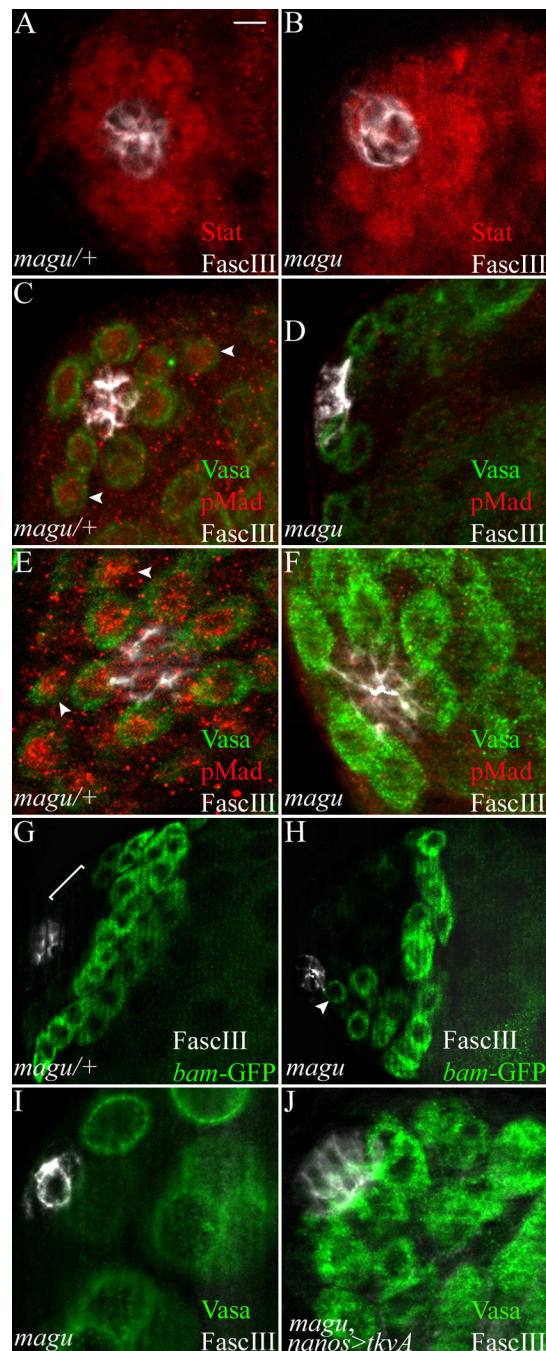
**Figure 5.**
BMP signaling is impaired in *magu* mutants. **(A)** *magu*/+ (*magu*deletionI/*CyOkr-Gal4UAS-GFP*). Anti-Stat showed accumulation of Stat protein (red) among the first tier of cells surrrounding the hub (FascIII, white). This reflects the normal activation of JAK/STAT pathway by hub signals. **(B)** *magu*deletionI/*magu*deletionI. The JAK-STAT pathway was activated (red) in cells surrounding the hub (white) as in control testes. **(C)** *magu*/+ (*magu*e00439 or f02256/*CyOkr-Gal4UAS-GFP*). The activation of BMP signaling was visualized by anti-phospho-Mad (pMad, red). We had difficulty consistently observing the reported pMad accumulation in germline cells (green) adjacent to the hub (white) in control

and wildtype testes. An example where we did observe a signal is shown. **(D)** *magu*[e00439]/*magu*[f02256]. We never observed pMad acumulation in mutant testes. **(E)** *magu*/+ (*magu*[deletionI]/*CyOkr-Gal4UAS-GFP*). In contrast to adult testes, in gonads from 3rd instar larvae we consistently observed pMad accumulation (red) in germ cells (green) adjacent to the hub (white). We noted that in larval gonads and those favorable preparations from adult testes with signals, pMad accumulation could also be observed in gonialblasts, not only in GSCs (C and E, arrowheads). **(F)** *magu*[deletionI]/*magu*[deletionI]. pMad accumulation was lost in mutant gonads. **(G)** *magu*/+ (*magu*[e00439] *bam-GFP/CyOkr-Gal4UAS-GFP*). Control testes showed no *bam* expression among the first few tiers of cells (bracket) adjacent to the hub (white). *bam* expression begins in germ cells at the late 2- into the 4-cell gonial stage. **(H)** *magu*[e00439] *bam-GFP/magu*[f02256]. In mutant testes *bam* expression was de-repressed in germ cells (green, arrowhead) adjacent to the hub (white). This was observed in all testes examined. **(I)** *magu*[e00439]/*magu*[f02256]. No germ cells (green) were directly attached to the hub (white) in this single focal section from a mutant testis. **(J)** *magu*[e00439]/*magu*[f02256]; *nanos*-Gal4/UAS-activated *thickvein* (*tkv*A). In mutant testes where the BMP pathway was activated in germ cells, GSC could be retained. Scale bar: 10 μm in G and H, 5 μm in other panels.

**Table 1**

*magu* affects GSC maintenance

| Condition | Genotype[a] | Median GSC # | IQR[b] | Min – Max[c] | P value[d] | % of Testes w/GSCs | P value[e] |
|---|---|---|---|---|---|---|---|
| 0–3 days, 25°C (unless noted) | magu[e] or [f] /CyO[f] | 8 (19)[g] | 8 – 10 | 6 – 13 | | 100 | |
| | magu[e] /magu[f] | 3 (21) | 2 – 4 | 0 – 7 | <0.01 | 76 | NA[h] |
| | magu[e] or [delI] /CyO | 7 (10) | 7 – 7.8 | 6 – 9 | | 100 | |
| | magu[e] /magu[delI] | 0 (10) | 0 – 1.5 | 0 – 6 | <0.01 | 30 | NA |
| | magu[KG delI] or [f] /CyO | 10 (10) | 9.3 – 11 | 8 – 12 | | 100 | |
| | magu[KG delI] /magu[f] | 2.5 (10) | 0 – 4 | 0 – 5 | <0.01 | 60 | NA |
| | magu[delI] /CyO[i] | 9 (13) | 7 – 10 | 6 – 13 | | 100 | |
| | magu[delI] / magu[delI][i] | 6 (10) | 5.3 – 7.8 | 4 – 9 | <0.01 | 100 | NA |
| | magu[eREV1] or [f] /CyO | 9 (8) | 8 – 9 | 5 – 10 | | 100 | |
| | magu[eREV1] /magu[f] | 7 (10) | 6 – 8 | 4 – 9 | <0.05 | 100 | NA |
| aged at 29°C for 3 days[j] | upd-Gal4; magu[e] /magu[f] ; MKRS | 0 (23) | 0 – 3.5 | 0 – 6 | | 43 | |
| | upd-Gal4; magu[e] /magu[f] ; UAS-V5-magu | 4 (21) | 3 – 5 | 1 – 7 | <0.01 | 100 | <0.01 |
| | upd-Gal4; magu[e] /magu[f] ; MKRS | 0 (27) | 0 – 3 | 0 – 6 | | 44 | |
| | upd-Gal4; magu[e] /magu[f] ; UAS-magu-Myc | 3 (25) | 0 – 4 | 0 – 8 | >0.1 | 64 | <0.05 |
| aged at 29°C for 12 days[j] | upd-Gal4; magu[e] /magu[f] ; MKRS | 0 (12) | 0 – 0.3 | 0 – 3 | | 25 | |
| | upd-Gal4; magu[e] /magu[f] ; UAS-V5-magu | 4 (12) | 2.8 – 4 | 2 – 5 | <0.01 | 100 | <0.01 |
| | upd-Gal4; magu[e] /magu[f] ; MKRS | 0 (11) | 0 – 0 | 0 – 0 | | 0 | |
| | upd-Gal4; magu[e] /magu[f] ; UAS-magu-Myc | 3 (17) | 2 – 4 | 0 – 5 | <0.01 | 94 | NA |
| 0–5 days, 25°C | magu[e] /magu[f] ; MKRS | 3 (18) | 2 – 4 | 0 – 6 | | 83 | |
| | magu[e] /magu[f] ; nanos-Gal4/UAS-magu-Myc | 4 (15) | 3 – 5 | 2 – 7 | <0.05 | 100 | >0.05 |
| | magu[e] /magu[f] ; MKRS | 2 (13) | 0 – 4 | 0 – 5 | | 62 | |

| Condition | Genotype[a] | Median GSC # | IQR[b] | Min – Max[c] | P value[d] | % of Testes w/GSCs | P value[e] |
|---|---|---|---|---|---|---|---|
| | magu[e] / magu[fl] ; nanos-Gal4/UAS-magu-GFP | 4 (17) | 3 – 4 | 2 – 6 | <0.05 | 100 | <0.01 |
| 0–3 days, 25°C | magu[e] / magu[fl] ; MKRS | 2.5 (16) | 0 – 4 | 0 – 6 | | 63 | |
| | magu[e] / magu[fl] ; nanos-Gal4/UAS-tkvA | 5 (25) | 3 – 6 | 1 – 8 | <0.01 | 100 | <0.01 |

[a] Alleles used: [e]=[e00439]; [f]=[f02256]; [eREV]= [revertant of e]; [del I]=[deletion I]; [KG del]=[KG deletion].

[b] Interquartile range = Quartile 3 - Quartile 1 (Q[3] - Q[1]); Q[3] = the 75th percentile, Q[1] = the 25th percentile).

[c] Minimum – Maximum, representing the spread of GSC numbers observed

[d] Calculated by Mann-Whitney test.

[e] Calculated by Chi-square test.

[f] CyO kr-Gal4 UAS-GFP

[g] Number of testes scored in parentheses

[h] Not Applicable

[i] GSC number scored in gonads from 3rd instar larvae.

[j] Animals (0–3 days of age) raised at 25°C were shifted to 29°C for 3 or 12 days.

**Table 2**

*magu* does not affect CySCs or hub cells

| | Genotype[a] | | P value (Student's T-Test) |
|---|---|---|---|
| | *magu*[e] /*magu*[f] | **Sibling Control** | |
| Average CySC number[b] | 21.7 ± 1.0 (16)[c] | 21.9 ± 1.0 (14) | >0.5 |
| S-phase index for CySCs[d] | 0.2 ± 0.03 (10) | 0.2 ± 0.01 (10) | >0.5 |
| Average hub cell number[e] | 9.6 ± 0.4 (20) | 9.9 ± 0.5 (17) | >0.5 |
| Average hub cell number[f] | 7.8 ± 0.5 (19) | 8.0 ± 0.5 (20) | >0.5 |

[a]Alleles used: [e]=[e00439]; [f]=[f02256]; Sibling control=*magu*[e] or [f] /*CyO kr-Gal4 UAS-GFP*

[b]CySC number was scored in 0–4 day adults at 25°C.

[c]Number of testes scored in parentheses

[d]The fraction of EdU+ Zfh1+ cells to total Zfh1+ cells, in 1–4 day adults at 25°C.

[e]Hub cell number was scored using FascIII and DNA staining, in 0–3 day adults at 25°C.

[f]Hub cell number was scored using Upd-Gal4 UAS-GFP and DNA staining, in 0–3 day adults grown at 25°C and aged at 29°C for 3 days.